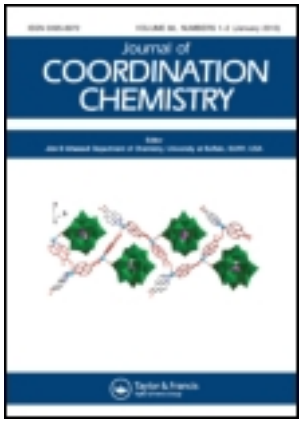

Journal of Coordination Chemistry
Publication details, including instructions for authors and subscription information:
http://www.tandfonline.com/loi/gcoo20

Construction and properties of drug molecules modifying octamolybdate hybrid compounds

Jing-Quan Sha[a], Pan Yang[a], Miao Chen[b], Chun-Jiang Li[a], Long-Jiang Sun[a] & Dong-Wen Wang[a]

[a] The Provincial Key Laboratory of Biological Medicine Formulation, School of Pharmacy, Jiamusi University, Jiamusi, P.R. China

[b] School of Pharmacy, Suzhou University, Suzhou, P.R. China

Accepted author version posted online: 16 Oct 2013.Published online: 15 Nov 2013.

To cite this article: Jing-Quan Sha, Pan Yang, Miao Chen, Chun-Jiang Li, Long-Jiang Sun & Dong-Wen Wang (2013) Construction and properties of drug molecules modifying octamolybdate hybrid compounds, Journal of Coordination Chemistry, 66:21, 3839-3847, DOI: 10.1080/00958972.2013.855304

To link to this article: http://dx.doi.org/10.1080/00958972.2013.855304

Journal of Coordination Chemistry, 2013
Vol. 66, No. 21, 3839–3847, http://dx.doi.org/10.1080/00958972.2013.855304

Construction and properties of drug molecules modifying octamolybdate hybrid compounds

JING-QUAN SHA*†, PAN YANG†, MIAO CHEN‡, CHUN-JIANG LI*†, LONG-JIANG SUN† and DONG-WEN WANG†

†The Provincial Key Laboratory of Biological Medicine Formulation, School of Pharmacy, Jiamusi University, Jiamusi, P.R. China
‡School of Pharmacy, Suzhou University, Suzhou, P.R. China

(*Received 13 June 2013; accepted 18 September 2013*)

By introducing antibacterial drug pipemidic acid into octamolybdates, two new compounds, $(HPPA)_4[Mo_8O_{26}]\ 2H_2O$ (**1**) and $[Ni_2(PPA)_2(H_2O)_4][Mo_8O_{26}]\ 3H_2O$ (**2**) (PPA = 8-ethyl-5,8-dihydro-5-oxo-2-(1-piperazinyl)pyrido(2,3-d)pyrimidine-6-carboxylic acid), have been synthesized and characterized by physical methods. Single-crystal X-ray analysis reveal that **1** and **2** crystallize in the triclinic system, space group *P-1*, in which supramolecular interactions play vital roles in stabilizing the structure of **1** and **2**. The results of their antitumor activities *in vitro* show that the compounds exhibit good anti-SGC7901 and anti-SMMC7721 activities, which indicates that the antitumor activities of Polyoxometalates can be modulated by the surface modification with drugs.

Keywords: Polyoxometalates; Octamolybdates; Quinolone antibacterial drugs; Antitumor activity

1. Introduction

Study of the interaction between drugs and transition metals/metal oxide clusters is an important and active research area in bioinorganic chemistry [1–4]. Action of many drugs is dependent on coordination with metal ions [1] or/and the inhibition [2] on the formation of metalloenzymes. Therefore, metals might play vital roles during the biological process of drug utilization in the body.

Polyoxometalates (POMs), as early-transition-metal oxide clusters, have become a large and appealing area in inorganic chemistry because of their versatile structures and numerous potential applications in catalysis, materials science, magnetism, and medicine [5–9]. POMs, as antitumor, antiviral, and antibacterial inorganic medical agents, are attractive for applications in medicine. Nearly, every molecular property, such as polarity, redox, surface charge distribution, shape, and acidity, that impacts the recognition and reactivity of POMs with target biological macromolecules can be altered easily. Also, the surface of POMs can be modified with multifunctional compounds by covalent attachment of organic groups. So design and synthesis of hybrid multifunctional materials based on POMs have gotten rapid

*Corresponding authors. Email: shajq2002@126.com (J.-Q. Sha); jmslcj@sohu.com (C.-J. Li)

growth, enriching the structures of POM-based hybrids but also ameliorating their properties [10–14]. The occurrence of metal-drug complexes modifying POMs is particularly rare [15–20], although many drugs have potential to act as ligands, and the resulting metal–drug complexes modifying POMs could be important in coordination chemistry and biochemistry.

Quinolone, quinolonecarboxylic acids, or 4-quinolones, are a group of synthetic antibacterial agents containing a 4-oxo-1,4-dihydroquinoline skeleton [scheme 1(a)]. Pipemidic acid (PPA) [scheme 1(b)], a 4-quinolone product, is an antibacterial agent used to treat gram-negative urinary tract infections [21] and severely damages DNA in the absence of an exogenous metabolizing system [22]. Due to the quinolone oxygen and one carboxylate oxygen, the PPA may act as an excellent multidentate ligand to coordinate with metal ions and further modify the POMs.

On the basis of the above considerations, we have chosen octamolybdates as modules and M-PPA/PPA as modifiers to constitute drug molecules modifying POM based compounds. We hope that isolated drug subgroups can be used to modulate POMs' properties and increase recognition of key substructures in target biomacromolecules. Herein, we report two new compounds based on octamolybdates, $(HPPA)_4[Mo_8O_{26}]\cdot 2H_2O$ (**1**) and $[Ni_2(PPA)_2(H_2O)_4]\cdot[Mo_8O_{26}]\cdot 3H_2O$ (**2**). The results of antitumor activity studies show that introduction of M-PPA/PPA onto the polyoxoanion surface can modulate their antitumor activities and make the compounds penetrate into the cells easily.

2. Experimental

2.1. *Materials and methods*

All reagents were purchased commercially and were used without purification. Elemental analyzes were performed on a Perkin–Elmer 2400 CHN (C, H, and N) and on a Leaman inductively coupled plasma spectrometer (Ni). IR spectra as KBr pellets were recorded on a Nicolet 170SX FTIR spectrophotometer from 400 to 4000 cm^{-1}. The TG analyzes were performed on a Perkin–Elmer TGA7 instrument in flowing N_2 at a heating rate of 10 °C min^{-1}.

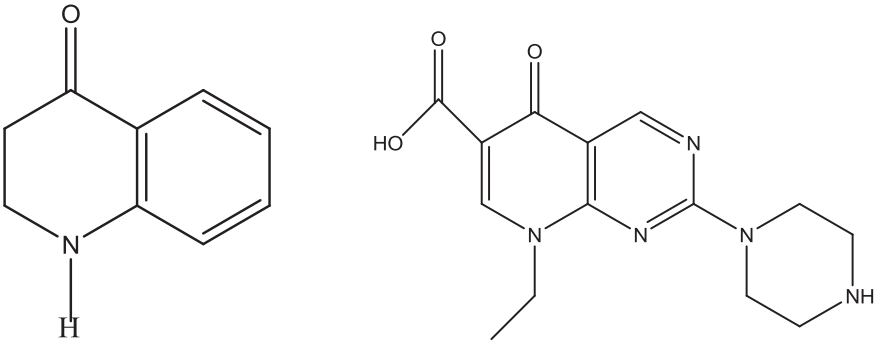

Scheme 1. (a) The 4-oxo-1,4-dihydroquinoline skeleton. (b) Pipedimic acid (8-ethyl-5,8-dihydro5-oxo-2-(1-piperazinyl)pyrido(2,3-d)pyrimidine-6-carboxylic acid = PPA).

2.2. *Syntheses*

2.2.1. $(HPPA)_4[Mo_8O_{26}]\cdot 2H_2O$ (1). A mixture of $(NH_4)_6Mo_7O_{24}\cdot 4H_2O$ (0.2 g, 0.16 mM), PPA (0.09 g, 0.3 mM), and H_2O (10 mL) was stirred at ambient temperature for 60 min, and the pH was adjusted to 4.0 with HNO_3 (1 M) solution and then transferred and sealed in an 18 mL Teflon-lined stainless steel container, which was heated at 160 °C for 96 h and then cooled to room temperature at a rate of 10 °C h^{-1}. Gray crystals of **1** were filtered and washed with distilled water (yield of 25% based on Mo). Anal. Calcd for $C_{56}H_{76}Mo_8N_{20}O_{40}$ (2436.9): C, 24.60; H, 3.12; N, 11.49 (%). Found: C, 24.54; H, 3.25; N, 11.48 (%).

2.2.2. $[Ni_2(PPA)_2(H_2O)_4]\cdot[Mo_8O_{26}]\cdot 3H_2O$ (2). A mixture of $(NH_4)_6Mo_7O_{24}\cdot 4H_2O$ (0.2 g, 0.16 mM), PPA (0.09 g, 0.3 mM), $Ni(NO_3)_2\cdot 6H_2O$ (0.3 g, 0.1 mM), and H_2O (10 mL) was stirred at ambient temperature for 60 min, and the pH was adjusted to 3.5 with HNO_3 (1 M) solution and then transferred and sealed in an 18 mL Teflon-lined stainless steel container, which was heated at 160 °C for 96 h and then cooled to room temperature at a rate of 10 °C h^{-1}. Green crystals of **2** were filtered and washed with distilled water (yield of 15% based on Mo). Anal. Calcd for $C_{28}H_{48}Mo_8N_{10}O_{39}Ni_2$ (2033.6): C, 16.53; H, 2.36; N, 6.88; Ni, 5.77 (%). Found: C, 16.48; H, 2.43; N, 6.18; Ni, 5.73 (%).

2.3. *X-ray crystallographic study*

Single-crystal X-ray diffraction data collections of **1** and **2** were performed using a Bruker Smart Apex CCD diffractometer with Mo-Kα radiation (λ = 0.71073 Å) at 293 K. Multi-scan absorption corrections were applied. All structures were solved by direct methods and refined by full-matrix least-squares on F^2 using the *SHELXTL* crystallographic software package [23]. The positions of hydrogens on carbon and nitrogen were calculated theoretically. A summary of the crystal data, data collection, and refinement parameters for **1** and **2** are listed in table 1. Selected bond lengths and angles for **1** and **2** are listed in tables S1 and S2. Crystallographic data for the structures reported in this paper have been deposited in the Cambridge Crystallographic Data Center.

2.4. *Antitumor activity studies*

The antitumor activity of **1** and **2** and their parent anion on SGC7901 cells was tested by the MTT experiment [24]. MTT is a dye which can accept a hydrogen. Surviving tumor cells are able to reduce the yellow MTT to an insoluble blue formazan in water whereas dead tumor cells do not possess this capability. The formazan product is dissolved in DMSO and then determined colorimetrically with a Microplate Reader (490 nm).

Subcultured SGC7901 cells were suspended in 0.25% trypsin. The cell suspension (*ca.* 10^5–10^6 cells mL) was added to a 96 well plate (100 μL per well) and incubated at 37 °C in a 5% CO_2 incubator for 24 h. The compounds containing 100 μL samples were then added. After 72 h, 20 μL MTT solution (5 mg mL^{-1} in 0.01 M PBS (phosphate buffer solution)) was added and the mixture allowed to incubate for 4 h. The supernatant was removed and DMSO (150 μL) added. The resulting mixture was shaken for 10 min at room temperature, and colorimetric analysis was used to examine the cell survival rate. These samples

Table 1. Crystal data and structure refinement for **1** and **2**.

Empirical formula	$C_{56}H_{76}Mo_8N_{20}O_{40}$	$C_{28}H_{48}Mo_8N_{10}O_{39}Ni_2$
CCDC	932966	932067
Formula weight	2436.9	2033.6
Temperature (K)	293	293(2)
Wavelength (Å)	0.71069	0.71069
Crystal system	Triclinic	Triclinic
Space group	*P-1*	*P-1*
a (Å)	10.372(5)	10.164(5)
b (Å)	11.161(5)	11.950(5)
c (Å)	18.961(5)	12.458(5)
α (°)	74.316(5)	95.827(5)
β (°)	88.169(5)	105.902(5)
γ (°)	80.138(5)	102.42(5)
V (Å^3)	2081.8(15)	1400.3(11)
Z	1	1
D_{Calcd} (mg/m^3)	1.944	2.409
Mu (mm^{-1})	1.267	2.496
F (0 0 0)	1208.0	988
Goodness-of-fit on F^2	1.078	1.189
Final *R* indices [$I > 2\sigma(I)$]	$R_1 = 0.0358$	$R_1 = 0.0242$
	$wR_2 = 0.1025$	$wR_2 = 0.0777$
R indices (all data)	$R_1 = 0.0534$	$R_1 = 0.0272$
	$wR_2 = 0.1280$	$wR_2 = 0.0914$

containing the title compounds and parent compound were obtained by dissolving the title compounds in DMSO, autoclaving and diluting by a RPMI 1640 medium to a final concentration of 200, 100, 50, 25, 12.5, 6.25, 3.13, and 1.56 μg mL^{-1}.

3. Results and discussion

3.1. *Crystal structures*

Bond valence sum calculations [25] show that all Mo ions in **1** and **2** are in the + VI oxidation state and Ni ions are in + II oxidation state (table S3). The results are consistent with coordination environments, crystal color, and formulas given by X-ray structure determination. In **1** and **2**, $[Mo_8O_{26}]^{4-}$ exhibits β-structural isomer with the most compact structure of eight edge-sharing $[MoO_6]$ octahedra with two $[Mo_4O_{13}]$ subunits stacking together [26, 27]. Thus, $[Mo_8O_{26}]^{4-}$ can be shortened as β-Mo_8 in the following description of structures.

3.1.1. Structure description of 1. Single-crystal X-ray diffraction analysis reveals that **1** consists of β-Mo_8, four protonated PPA cations and two waters as shown in figure 1(a). To balance the charge, one proton is added to PPA because of the stronger basicity of the terminal nitrogen than that of oxygen of β-Mo_8. Supramolecular interactions play vital roles in stabilizing the structure of **1** (table 2). For example, each β-Mo_8 links the adjacent eight PPA molecules through short interactions with O5···C4 (3.20 Å), O12···C15 (3.08 Å), O5···N1 (2.885 Å), O1···N1 (2.890 Å), O12···N6 (2.953 Å), O10···N6 (2.954 Å), and O3···N6 (3.005 Å) shown in figure 1(b). In turn, each PPA links the neighboring β-Mo_8 cluster and PPA ligand via short interactions C6···C24 (3.261 Å), C22···C25 (3.303 Å), and

C23···C26 (3.256 Å) shown in figure 1(c). As a result, β-Mo_8 and PPA molecules connect forming the supramolecular 3-D structure.

3.1.2. Structure description of 2. Single-crystal X-ray diffraction analysis reveals that **2** consists of an isolated Ni-PPA coordination subunit $[Ni_2(PPA)_2(H_2O)_4]^{2+}$, a β-$Mo_8$ and three waters as shown in figure 2(a). There are two crystallographically independent Ni^{II} centers. Ni1 shows an octahedral geometry configuration with its two axial sites bonding to two β-Mo_8 clusters (Ni1–O12 = 2.048 Å) and with its equatorial sites bonding to four oxygens from two different PPA ligands (Ni1–O14 = 2.043 Å) and two waters (Ni1O1W = 2.165 Å). Ni2 is six-coordinate by four oxygens from two PPA ligands (Ni2O = 1.986–1.992 Å) and two waters (Ni2–O2W = 2.086 Å). The octamolybdate polyoxoanion as a bidentate ligand connects two Ni ions forming a 1-D POM-metal inorganic chain [figure 2(b)]. Ni1 centers are bridged by PPA ligands via two hydroxyl groups to form an interesting 1-D organic–inorganic hybrid chain [figure 2(c)]. As a result, two types of chains are intersected via Ni1 to construct a 2-D sheet [figure 2(d)]. The 2-D layers are stacked in a parallel fashion to form a 3-D structure through supramolecular interactions.

3.2. *IR spectra and TG analyzes*

The IR spectra for **1** and **2** are presented in figure S1. The bands at 920–650 cm^{-1} are ascribed to υ(Mo=O) and υ(Mo–O–Mo). A series of medium intensity bands at 1630–1030 cm^{-1} are associated with quinolone. Spectra of the two compounds are very similar in the M–O stretching vibration region with a slight difference, perhaps due to the structural difference [28].

As shown in figure S2, the thermal analysis of **1** gives a total loss of 51.5% from 40 to 660 °C, ascribed to removal of two lattice waters (Calcd 1.47%) and decomposition of PPA

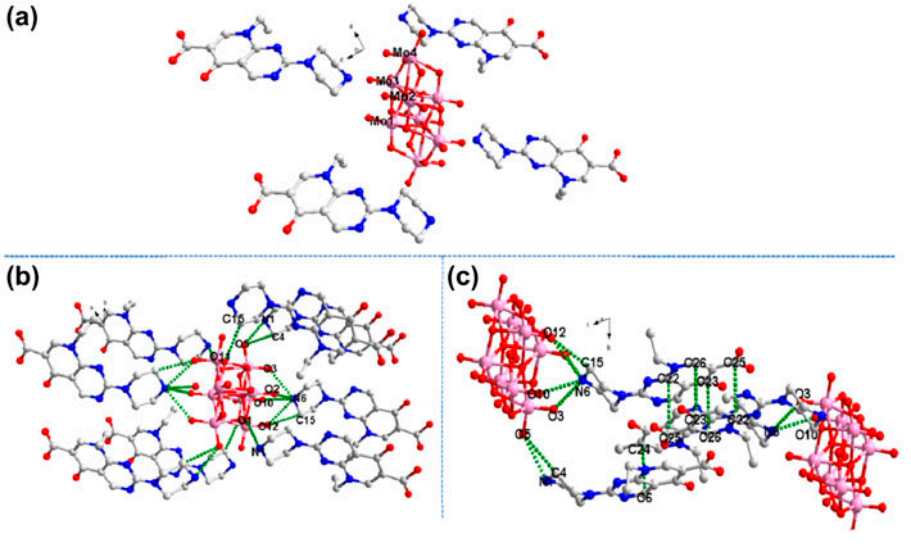

Figure 1. (a) Ball/stick representation of the molecular structure of **1**. All hydrogens and waters have been omitted for clarity. (b) and (c) ball/stick representation of supramolecular interactions among β-Mo_8 and PPA.

Table 2. Supramolecular interactions of **1**.

Interaction	Distance (Å)	Interaction	Distance (Å)	Interaction	Distance (Å)
O3···H4B–C4	2.589	O3···H7A–C7	2.599	O3···H6A–C6	2.588
O3···N6	3.005	O10···H6A–N6	2.274	O10···N6	2.945
O2···N6	3.054	O2···H6B–N6	2.274	O2···H2A–C2	2.609
O12···H3B–C3	2.509	O12···H15A–C15	2.660	O12···C15	3.082
O12···N6	2.952	O12···H6B–N6	2.271	O1···H9B–N1	1.991
O5···H9B–N1	2.668	O5···H9B–N1	2.654	O5···C4	3.201
O5···N1	2.885	O15···H1A–C1	2.524	O18···H17B–C17	2.669
O17···H17B–C17	2.547	O1···N1	2.890	O10···N6	2.954
C6···C24	3.261	C9···C9	3.355	H12B···H18B–C18	2.302

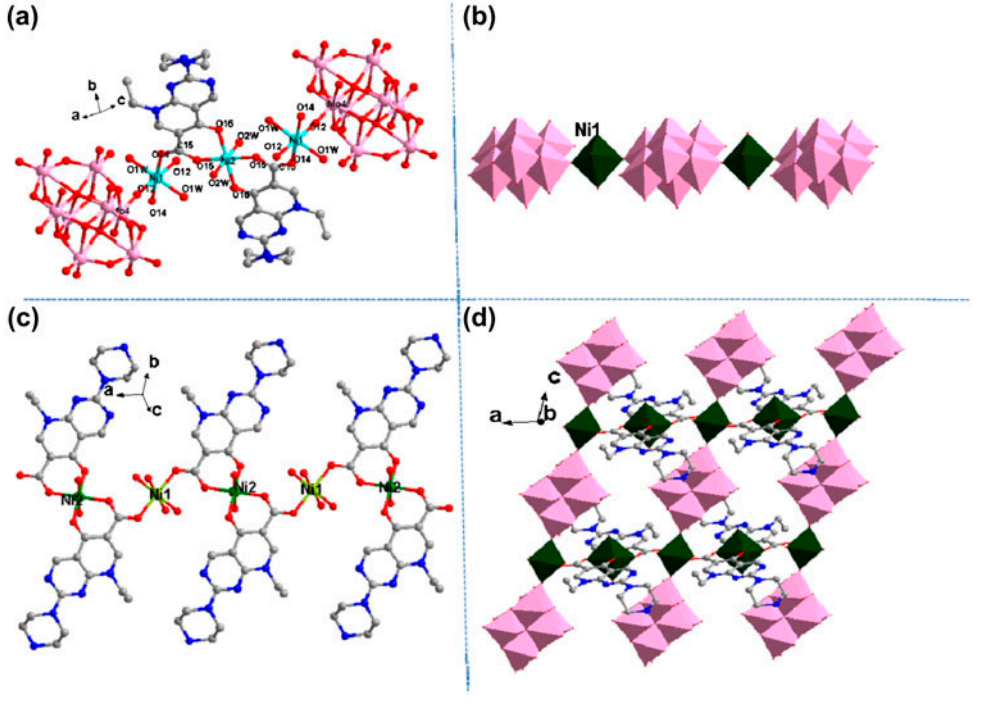

Figure 2. (a) Stick/ball representation of the asymmetric unit of **2**. Only some atoms are labeled, and all hydrogens are omitted for clarity. (b) 1-D POM-metal inorganic chain. (c) 1-D drug-metal complex chain. (d) 2-D layer structure constructed by β-Mo_8 and drug-metal complex chain.

(Calcd 49.74%). The result agrees with the calculated weight loss of 51.2%. The TG curve of **2** shows similar weight loss process to **1**. The whole weight loss (36.06%) is in agreement with the calculated value (35.99%) from 40 to 670 °C with removal of three lattice waters (Calcd 2.65%), four coordinated waters (Calcd 3.54%), and decomposition of PPA (Calcd 29.8%). These results further confirm the formulas of **1** and **2**.

3.3. *Antitumor activity studies*

A comparison of the antitumor activities on SGC7901 and SMMC7721 cells for **1** and **2** and their parent β-Mo_8 was made. The inhibitory effect against SGC7901 and SMMC7721 lines

shows that **1** and **2** exhibit higher antitumor activities, while the parent compound shows anti-SGC7901 activity, but no anti-SMMC7721 activities as shown in figure 3. The inhibitory effective cell 50% lethal concentration (IC_{50}) against SGC7901 and SMMC7721 cells (table 3) shows that the values of IC_{50} for β-Mo_8, **1** and **2** are 345, 184, and 169 μg/mL for SGC7901 and 296 and 337 μg/mL for SMMC7721, respectively. The differences can be reasonably explained by the modifying chemistry of POMs. The introduction of PPA/M-PPA onto the POM surface can ameliorate POMs' electronic distribution, polarity, and redox potentials so that recognition and reactivity of POMs with target biological macromolecules can be altered, resulting in their antitumor activity. Firstly, comparing **1** and **2** with parent, after β-Mo_8 clusters are modified by PPA/M-PPA, the nature of POMs is affected by the

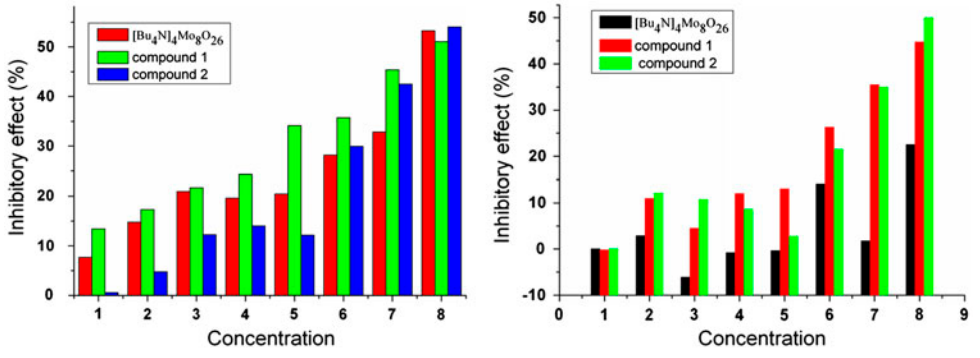

Figure 3. Histogram of the anti-tumor activity against SGC7901 (left) and SMMC7721 (right) about **1**, **2** and the parent compound.

Table 3. Inhibitory effect of **1**, **2** and parent compound on tumor cells *in vitro*.

Compounds	Dose (μg/mL)	RI% (SGC7901)	RI% (SMMC7721)	IC_{50} (μg/mL)
$[Bu_4N]_4$ Mo_8O_{26}	200	53.27	22.53	345 (SGC7901)–(SMMC7721)
	100	32.84	1.79	
	50	28.18	14.09	
	25	20.48	−0.36	
	12.5	19.62	−0.79	
	6.25	20.97	−6.08	
	3.125	14.78	2.93	
	1.5625	7.69	0.07	
Compound **1**	200	51.05	44.74	184 (SGC7901) 297 (SMMC7721)
	100	45.39	35.50	
	50	35.71	26.26	
	25	34.14	13.05	
	12.5	24.29	12.03	
	6.25	21.71	4.55	
	3.125	17.31	11.00	
	1.5625	13.41	−0.15	
Compound **2**	200	54.05	50	170 (SGC7901) 337 (SMMC7721)
	100	42.49	34.98	
	50	29.96	21.53	
	25	12.19	2.79	
	12.5	14.00	8.66	
	6.25	12.27	10.80	
	3.125	4.78	12.09	
	1.5625	0.61	0.07	

supramolecular interaction and covalent bond, which results in the change in antitumor activity. **1** and **2** make the anti-SMMC7721 activity of β-Mo_8 be activated. Comparing **1** and **2**, the antitumor activities of **2** are higher than that of **1**. The difference may rest on the differences of their structures, namely, PPA drug subunits surround the Mo_8 clusters via noncovalent interactions, which result in less effect on the properties of POMs; Ni-PPA subunits covalently linking to Mo_8 clusters may bring a bigger effect on the properties of POMs in **2**. To some extent, the result indicates that enhanced antitumor activities may arise from Ni ions, promoting transition of electrons between POMs and PPA drugs.

4. Conclusions

Two PPA-M/PPA-β-Mo_8 based compounds were obtained and structurally characterized. The MTT investigations find that the two new compounds possess better antitumor activity than the parent due to property change of β-Mo_8. Thus, modification of POMs can affect electron transfer between POMs and PPA drugs, which in turn affects their antitumor activities. Combined with reported work, we can deduce that the changes of antitumor properties come from the synergism of POMs, metal ions drug molecules, and the final structure. Isolation of the two compounds is helpful to explore the possible effect of drug molecules modifying POM clusters.

Supplementary material

CCDC (932966 and 932067) contains the supplementary crystallographic data for **1** and **2**, respectively. These data can be obtained free of charge via http://www.ccdc.cam.ac.uk/conts/retrieving.html, or from the Cambridge Crystallographic Data Center, 12 Union Road, Cambridge CB2 1EZ, UK; Fax: (+44) 1223-336-033; or E-mail: deposit@ccdc.cam.ac.uk. Tables of selected bond lengths (Å), bond angles (deg) and IR and TG for **1** and **2** are provided in supporting information http://dx.doi.org/10.1080/00958972.2013.855304.

Acknowledgments

This work was financially supported by the the training program for New Century Excellent Talents in universities (1253-NCET-022) in Heilongjiang Province.

References

[1] A. Albert. *The Physico–Chemical Basis of Therapy: Selective Toxicity*, 6th Edn, Chapman & Hall, London (1979).
[2] M.N. Hughes (Ed.). *The Inorganic Chemistry of Biological Processes*, 2nd Edn, Wiley, New York (1981).
[3] A. Tarushi, C.P. Raptopoulou, V. Psycharis, A. Terzis, G. Psomas, D.P. Kessissoglou. *Bioorg. Med. Chem.*, **18**, 2678 (2010).
[4] M.N. Patel, P.A. Parmar, D.S. Gandhi. *Bioorg. Med. Chem.*, **18**, 1227 (2010).
[5] D.L. Long, E. Burkholder, L. Cronin. *Chem. Soc. Rev.*, **36**, 105 (2007).
[6] P.P. Mishra, J. Pigga, T.B. Liu. *J. Am. Chem. Soc.*, **130**, 1548 (2008).
[7] S.D. Jiang, B.W. Wang, G. Su, Z.M. Wang, S. Gao. *Angew. Chem. Int. Ed.*, **10**, 1736 (2010).
[8] T. Ishida, M. Nagaoka, T. Akita, M. Haruta. *Chem. Eur. J.*, **14**, 8456 (2008).
[9] X. Wang, J. Liu, M.T. Pope. *Dalton Trans.*, **957** (2003).
[10] G.F. Swiegers, T.J. Malefetse. *Chem. Rev.*, **100**, 3483 (2000).
[11] D.F. Sun, D.J. Collins, Y.X. Ke, J.L. Zuo, H.C. Zhou. *Chem. Eur. J.*, **12**, 3768 (2006).
[12] Y. Wang, X.Q. Zhao, W. Shi, P. Cheng, D.Z. Liao, S.P. Yan. *Cryst. Growth Des.*, **9**, 2137 (2009).
[13] H. Abbas, C. Streb, A.L. Pickering, A.R. Neil, D.L. Long, L. Cronin. *Cryst. Growth Des.*, **8**, 635 (2008).

[14] J.Q. Sha, J. Peng, H.S. Liu, J. Chen, A.X. Tian, P.P. Zhang. *Inorg. Chem.*, **46**, 11183 (2007).
[15] X. Wang, J. Liu, J. Li, Y. Yang, J. Liu, B. Li, M.T. Pope. *J. Inorg. Biochem.*, **94**, 279 (2003).
[16] H. Zhang, Y. Lan, L.Y. Duan. *J. Coord. Chem.*, **56**, 85 (2003).
[17] J. Li, Y.F. Qi, H.F. Wang, E.B. Wang, C.W. Hu, L. Xu, X.Y. Wu. *Chem. J. Chin. Univ.*, **25**, 1010 (2004).
[18] H.Y. An, D.R. Xiao, E.B. Wang, Y.G. Li, Z.M. Su, L. Xu. *Angew. Chem. Int. Ed.*, **45**, 904 (2006).
[19] J.Q. Sha, Y.H. Zhang, L.Y. Liang, H.B. Qiu, M.Y. Liu. *J. Coord. Chem.*, **65**, 3264 (2012).
[20] J.-Q. Sha, L.-Y. Liang, P.-F. Yan, G.-M. Li, C. Wang, D.-Y. Ma. *Polyhedron*, **31**, 422 (2012).
[21] K.G. Naber. *J. Antimicrob. Chemother.*, **46**, 49 (2000).
[22] V.M. Sundermann, K.H. Hauff, P. Braun, W. Lu. *Int. J. Oncol.*, **5**, 855 (1994).
[23] (a) G.M. Sheldrick, SHELX-97, Program for Crystal Structure Refinement, University of Göttingen, Göttingen (1997); (b) G.M. Sheldrick, SHELXL-97, Program for Crystal Structure Solution, University of Göttingen, Göttingen (1997).
[24] X.H. Wang, J.F. Liu, Y.G. Chen, Q. Liu, J.T. Liu, M.T. Pope. *J. Chem. Soc., Dalton Trans.*, 1139 (2000).
[25] I.D. Brown, D. Altermatt, *Acta Crystallogr., Sect. B: Struct. Sci*, **41**, 244 (1985).
[26] Y.-Q. Lan, S.-L. Li, X.-L. Wang, K.-Z. Shao, D.-Y. Du, H.-Y. Zang, Z.-M. Su. *Inorg. Chem.*, **47**, 8179 (2008).
[27] H. Abbas, C. Streb, A.L. Pickering, A.R. Neil, D.L. Long, L. Cronin. *Cryst. Growth Des.*, **8**, 635 (2008).
[28] A.X. Tian, X.L. Lin, G.Y. Liu, R. Xiao, J. Ying, X.L. Wang. *J. Coord. Chem.*, **66**, 1340 (2013).